Int. J. Solids Structures, 1970, Vol. 6, pp. 871 to 892. Pergamon Press. Printed in Great Britain

ANALYSIS OF THE TRANSIENT EXCITATION OF AN ELASTIC ROD BY THE METHOD OF CHARACTERISTICS

Y. MENGI† and H. D. MCNIVEN‡

University of California, Berkeley, California 94720

Abstract—The response of a semi-infinite, isotropically elastic rod to a time dependent input on the end of the rod is found using the method of characteristics. To reduce the problem to one where motions depend on only one space variable and time the approximate theory for rods due to Mindlin and McNiven is used. The response is found at stations near the end of the rod to a step input of pressure and is compared to the responses reported in other published works and to a response found independently by the authors.

1. INTRODUCTION

THE response of a circular, semi-infinite, isotropically elastic rod to time dependent conditions on its end is a problem that has attracted a great deal of attention over the period of the last fifteen years. It is a difficult problem and even though the studies to date have been important there is much about the response of the rod that remains unknown. Most of what is known concerns the response at stations far from the end of the rod. These responses have been formulated using the exact three dimensional theory and integral transforms and the integrals have been evaluated using the method of steepest descent. This method limits the results to "large" values of the space variable dictating distant stations. Even at these distant stations we have information only about the head of impulse and no information behind it.

The first study was made by Skalak [1] who formulated the problem using the exact three-dimensional theory and found the response to a step input of velocity on the end of the rod. He obtained an asymptotic solution for the head of impulse by representing the frequency equation as the first two terms of a Taylor expansion about the origin of the frequency–wave number plane.

Folk *et al.* [2] formulated the problem much the same as Skalak except that they used mixed–mixed conditions on the end of the rod including a step input of pressure. Their approximation of the integrals was also much the same as Skalak. Their most valuable contribution was in suggesting a possible method, using saddle point, for finding information about the response at distances behind the head of impulse.

Kaul and McCoy [3] developed the problem differently in that instead of the exact theory they used the approximate theory due to Mindlin and McNiven [4].

Jones and Norwood [5] extended the method of Skalak by using three terms of the Taylor expansion for the frequency equation rather than two. They claim that the additional term improves the solution for the head of impulse.

† Research Assistant.
‡ Professor of Engineering Science.

Lloyd and Miklowitz [6] further refined the technique by taking into account the contributions from higher branches; real, imaginary and complex. Though their study was directed to the response in plates, their method is equally applicable to rods.

There have been two previous studies that do not suffer the shortcomings inherent to the method of steepest descent. Both have used a method that restricts finding the response close to the end of the rod and have shown not only the head of impulse but the behavior behind the head.

The first of these is due to Miklowitz [7]. He formulated his problem in integral transforms but used an ingenious method for numerical integration that enabled him to find the response near the end of the rod. His study is based on an approximate theory and unfortunately at the time of the study the best theory available was due to Mindlin and Herrmann [8] so in using it his results reflect the shortcomings of that theory. The Mindlin–Herrmann theory takes into account the fundamental mode of steady state vibration and one higher mode that is identified as the radial mode. Later, a study of the same problem by Mindlin and McNiven [4] showed that for realistic values of Poisson's ratio this radial mode is strongly coupled to a third mode identified by them as the first axial shear mode. In addition, this later study described a critical value of Poisson's ratio and noted that for values of Poisson's ratio below this value the second mode is indeed the radial mode but that for values of Poisson's ratio above this critical value the radial mode is no longer the second but is the third mode. The influence of the Mindlin–Herrmann theory on the numerical results obtained by Miklowitz is discussed in the section on numerical analysis.

The second study was made by Bertholf [9] who used the exact three dimensional theory of elasticity and solved the equations using finite differences. Our reservation about his work has to do with a mathematical weakness in his numerical analysis. Bertholf apparently did not take into account the notion of the domain of dependence for hyperbolic equations which puts a restriction on the selection of the time mesh size as a function of the space mesh size.

In the method to be developed here we are able to exploit two circumstances. First, the equations governing the propagation of waves in an elastic rod are hyperbolic, and second, the lines on the time-space plane that locate wave fronts coincide with characteristic lines. The method of characteristics is really only practical in solving problems with two independent variables and so we have used an approximate theory instead of the three dimensional theory for the propagation of waves. As we are dealing with circular rods, our choice is the theory due to Mindlin and McNiven [4]. This theory allows for frequencies below the cut-off frequency of the second axial shear mode and in the frequency range permitted, the predictions from this theory match accurately the predictions from the three-dimensional theory.

Using the method of characteristics one is able to reduce the Mindlin–McNiven equations to two types of equations. The first type is the decay equation which is integrated directly on the space–time plane to find the behavior on the first wave front. We explore the domain beyond the first wave front by means of the canonical form of the governing equations. These are valid along characteristic lines and are integrated using finite differences.

The method has many advantages. The conditions on the end of the rod can be any mixture of conditions including those that can be realized experimentally and the time dependency can be arbitrary. The response is found near the end of the rod where it is likely to be of most interest. From what we can ascertain, short of doing our own experiments,

the response is accurate. The Mindlin–McNiven theory is used to its full capacity throughout the numerical analysis. We show that our numerical analysis is convergent, that is we show that as the mesh size goes to zero, so do the error.

There are perhaps two shortcomings of the method. First, if one desires the response at stations far from the end of the rod, or at distances far behind the head of impulse, a lot of computer time would be needed. This is true not only because the response would be needed far from the origin of the space–time plane where the numerical analysis originates, but the mesh size would have to be small to obtain accurate results.

The Mindlin–McNiven equations predict no decay of axial strain along the line representing the first wave front whereas intuition tells us there will be decay.

The method of characteristics is not entirely new to the problem of wave propagation in rods. Tang [10] used characteristics along with the Mindlin–Herrmann theory to obtain the average stress response P_z at stations close to the end of the rod.

2. METHOD OF CHARACTERISTICS FOR A SYSTEM OF LINEAR, SECOND-ORDER, PARTIAL DIFFERENTIAL EQUATIONS

The general method of characteristics is by this time classical knowledge and so will not be reviewed here. What will be studied is a particular set of differential equations which accommodates equations due to Mindlin and McNiven [4] which in turn govern approximately the axisymmetric motions in isotropically elastic rods. The study will show that these governing equations are substantially simplified when put into canonical form along characteristic lines, simplifications that lend themselves to numerical analysis.

The particular set of differential equations treated here has been studied by P. C. Chou and R. W. Mortimer [11] and their canonical equations are the same as those developed here. The same results could have been arrived at using a general method by Courant and Hilbert [12] who first reduce higher order equations to first order equations and then establish the canonical form of the equations along characteristics. Of the alternatives our preference is for the method presented here as it is systematic and simple.

We consider a set of differential equations of the form

$$u_{i,xx} - \frac{1}{c_i^2} u_{i,tt} = \alpha_{ij} u_j + \beta_{ij} u_{j,x} \qquad (i = 1, \ldots, n). \tag{1}$$

In equation (1) $u_i = u_i(x, t)$ but the c_i, α_{ij}, β_{ij} are continuous functions of x only. The usual rules of indicial notation hold, i.e. $u_{,x} = \partial u/\partial x$ etc; and repeated indices indicates summation except that there is no sum on i.

Since $u_i = u_i(x, t)$, we will consider the behavior of each u_k over the x–t plane. As the dependent variables in the Mindlin–McNiven equations represent displacements, physical considerations dictate that the u_i's themselves will be continuous. However, we allow all of the partial derivatives of the u_i to suffer finite discontinuities. The lines across which these discontinuities occur will be called characteristic lines and will be designated as $x = \tilde{x}(t)$. We will enclose a function by square brackets to denote the finite jump of the function across a characteristic line, i.e. $[f]$ designates the finite jump of the function (f) across $x = \tilde{x}(t)$. The order of the discontinuity will match the order of the derivative suffering the jump. We now proceed to establish the equations of the characteristics for each order of discontinuity, and begin with the second order as it is the simplest.

(a) *Second order discontinuities*

For this order

$$\begin{aligned} &[u_i] = [u_{i,x}] = [u_{i,t}] = 0, \\ &[u_{i,xx}] \neq 0, \qquad [u_{i,tt}] \neq 0, \qquad [u_{i,xt}] \neq 0 \quad \text{along } x = \tilde{x}(t). \end{aligned} \tag{2}$$

On both sides of $x = \tilde{x}(t)$, equation (1) is satisfied. If we write equation (1) for both sides of $x = \tilde{x}(t)$ and take the difference, we get

$$[u_{i,xx}] - \frac{1}{c_i^2}[u_{i,tt}] = 0 \tag{3}$$

along $x = \tilde{x}(t)$.

Here we use Hadamard's lemma which states "that $[f] = 0$ along $x = \tilde{x}(t)$ implies $[f_{,t}] + (\mathrm{d}\tilde{x}/\mathrm{d}t)[f_{,x}] = 0$". We apply the lemma to each of the first derivatives to obtain:

$$[u_{i,tt}] = \left(\frac{\mathrm{d}\tilde{x}}{\mathrm{d}t}\right)^2 [u_{i,xx}]. \tag{4}$$

Substitution of equation (4) in equation (3) gives

$$\left\{1 - \frac{1}{c_i^2}\left(\frac{\mathrm{d}\tilde{x}}{\mathrm{d}t}\right)^2\right\}[u_{i,xx}] = 0. \tag{5}$$

But by definition, $[u_{i,xx}] \neq 0$, so

$$\frac{\mathrm{d}\tilde{x}}{\mathrm{d}t} = \pm c_i, \tag{6}$$

the equations for the families of lines along which second order discontinuities occur.

(b) *First order discontinuities*

For this order.

$$\begin{aligned} &[u_i] = 0 \\ &[u_{i,t}] \neq 0; \qquad [u_{i,x}] \neq 0 \end{aligned} \tag{7}$$

along $x = \tilde{x}(t)$, and on both sides of $x = \tilde{x}(t)$ equation (1) is satisfied.

As before we use Hadamard's lemma; this time with the dependent variables themselves. The resulting equation is

$$[u_{i,t}] = -\frac{\mathrm{d}\tilde{x}}{\mathrm{d}t}[u_{i,x}]. \tag{8}$$

As equation (1) is of second order, and we are dealing with first order discontinuities, we put equation (1) in the form of an integral equation;

$$\int_a^b u_{i,xx}\,\mathrm{d}x - \frac{1}{c_i^2}\frac{\partial}{\partial t}\int_a^b u_{i,t}\,\mathrm{d}x = \int_a^b \alpha_{ij}u_j\,\mathrm{d}x + \int_a^b \beta_{ij}u_{j,x}\,\mathrm{d}x. \tag{9}$$

Equation (9) can be written

$$u_{i,x}(b,t) - u_{i,x}(a,t) - \frac{1}{c_i^2}\frac{\partial}{\partial t}\int_a^b u_{i,t}\,\mathrm{d}x = \int_a^b (\alpha_{ij} - \beta_{ij,x})u_j\,\mathrm{d}x + \beta_{ij}(b)u_j(b,t) - \beta_{ij}(a)u_j(a,t). \tag{10}$$

We now suppose that the interval $[a, b]$ encloses $x = \tilde{x}(t)$, i.e. $a < x = \tilde{x}(t) < b$, so that the interval may be divided into two parts namely $[a, \tilde{x}^-(t)]$ and $[\tilde{x}^+(t), b]$.

Accordingly we can write equation (10) as

$$u_{i,x}(b,t)-u_{i,x}(a,t)-\frac{1}{c_i^2}\left\{\frac{\partial}{\partial t}\int_a^{\tilde{x}^-} u_{i,t}\,dx+\frac{\partial}{\partial t}\int_{\tilde{x}^+}^b u_{i,t}\,dx\right\}$$

$$=\int_a^b(\alpha_{ij}-\beta_{ij,x})u_j\,dx+\beta_{ij}(b)u_j(b,t)-\beta_{ij}(a)u_j(a,t),$$

or

$$u_{i,x}(b,t)-u_{i,x}(a,t)-\frac{1}{c_i^2}\left\{u_{i,t}(\tilde{x}^-,t)\frac{d\tilde{x}^-}{dt}+\int_a^{\tilde{x}^-} u_{i,tt}\,dx-u_{i,t}(\tilde{x}^+,t)\frac{d\tilde{x}^+}{dt}+\int_{\tilde{x}^+}^b u_{i,tt}\,dx\right\}$$

$$=\int_a^b(\alpha_{ij}-\beta_{ij,x})u_j\,dx+\beta_{ij}(b)u_j(b,t)-\beta_{ij}(a)u_j(a,t). \tag{11}$$

We now assume that $x = \tilde{x}(t)$ is a continuous and differentiable curve on the x–t plane, so $d\tilde{x}^-/dt = d\tilde{x}^+/dt = d\tilde{x}/dt$. We shrink the interval $[a, b]$ to a point so that "a" approaches x from the left and "b" approaches from the right. For this case equation (11) reduces to

$$[u_{i,x}]+\frac{1}{c_i^2}[u_{i,t}]\frac{d\tilde{x}}{dt}=0. \tag{12}$$

If we substitute equation (8) in equation (12) we find

$$\left\{1-\frac{1}{c_i^2}\left(\frac{d\tilde{x}}{dt}\right)^2\right\}[u_{i,x}]=0. \tag{13}$$

As $[u_{i,x}] \neq 0$,

$$\frac{d\tilde{x}}{dt}=\pm c_i \tag{14}$$

are the lines for first order discontinuities.

(c) *Comments on characteristics*

For the particular set of differential equations of equation (1) we see that first and second order discontinuities occur along the same set of lines called characteristics. Indeed it is simple to show by the method of part (a) that all higher order discontinuities, if they occur, will do so along the same set of characteristics.

Examination of equations (6) and (14) shows that when the c_i's are constants the characteristics will be straight lines. It is also well known that when the differential equations are hyperbolic, as ours are, the c_i's are real.

Corresponding to each differential equation there will be two families of characteristics on the (x–t) plane, a family with the slope c_k and a family with the slope $(-c_k)$. Because of the nature of the set of equations (1) the dependent variables u_i will be coupled by the lower order terms on the right side of the equations. One can also observe from equations (5) and (13) that when a particular characteristic line accommodates a jump in a number of derivatives of one dependent variable, the lowest order derivative of those suffering a jump will be uncoupled.

(d) *Canonical form of the differential equation*

Along characteristic lines equations (1) are considerably simplified. To get the simplified or canonical form we begin by writing equations (1) in the form

$$+c_i u_{i,xx} - \frac{1}{c_i} u_{i,tt} = +c_i(\alpha_{ij}u_j + \beta_{ij}u_{j,x})$$

and into this we substitute the equation of the characteristic either equations (6) or (14), giving

$$\mp\frac{dx}{dt}u_{i,xx} \pm \frac{dt}{dx}u_{i,tt} = \mp\frac{dx}{dt}(\alpha_{ij}u_j + \beta_{ij}u_{j,x}). \tag{15}$$

Equation (15) can be written

$$\left(\mp\frac{dx}{dt}u_{i,xx} \mp u_{i,xt}\right) \pm \left(u_{i,xt} + \frac{dt}{dx}u_{i,tt}\right) = \mp\frac{dx}{dt}(\alpha_{ij}u_j + \beta_{ij}u_{j,x})$$

which in turn can be written

$$\mp\frac{d}{dt}(u_{i,x}) \pm \frac{dt}{dx}\frac{d}{dt}(u_{i,t}) = \mp\frac{dx}{dt}(\alpha_{ij}u_j + \beta_{ij}u_{j,x})$$

or

$$\mp d(u_{i,x}) - \frac{1}{c_i}d(u_{i,t}) = \mp dx(\alpha_{ij}u_j + \beta_{ij}u_{j,x}). \tag{16}$$

Equation (16) is the canonical form of equations (1) along $dx/dt = \mp c_i$ respectively and in it $i, j = 1, \ldots, n$, with no sum on i. To use this equation the first derivative must be continuous and differentiable along the characteristic but second and higher order discontinuities are permitted. The equations are particularly useful as they lend themselves to numerical analysis, a fact that will be displayed in a later section.

(e) *Decay equations for first order discontinuities*

Since first order discontinuities are not permitted with the use of equations (16) and they are admitted in the theory there must be a special method of dealing with them. For first order discontinuities we develop decay equations. They are developed from equations (16) by recognizing that even though the equations are not valid along the characteristic itself, they are valid on each side of it. The decay equations are used to calculate the changes in the discontinuities of the first derivatives from station to station. The decay will depend on both the initial and boundary conditions.

As there are two families of characteristics $dx/dt = +c_i$ and $dx/dt = -c_i$, each will be treated separately.

(1) *Along* $dx/dt = c_i$. We begin by using equations (16) with the choice of the lower sign on each side of the equations. We assume that $u_{i,x}$ and $u_{i,t}$ are continuous and differentiable on both sides of a characteristic, and write equations (16) on either side of a characteristic line and take the difference. We obtain

$$\frac{d}{dx}[u_{i,x}] - \frac{1}{c_i}\frac{d}{dx}[u_{i,t}] = \beta_{ii}[u_{i,x}]. \tag{17}$$

In this equation and in all of what follows there is no summation on the i's. Since $[u_i] = 0$ along the characteristic we have from equation (8)

$$[u_{i,t}] = -\frac{dx}{dt}[u_{i,x}] = -c_i[u_{i,x}]. \tag{18}$$

Substituting (18) into (17) gives

$$\frac{d}{dx}[u_{i,x}]+\frac{1}{2}\left(\frac{1}{c_i}\frac{dc_i}{dx}-\beta_{ii}\right)[u_{i,x}] = 0. \tag{19}$$

Integrating equation (19), we find

$$[u_{i,x}] = K_i c_i^{-\frac{1}{2}} e^{\frac{1}{2}\int \beta_{ii}\,dx} \tag{20}$$

The K_i's are constants to be determined from the boundary and initial conditions. Employing equation (18) in this same way we find the decay equations for the discontinuity of $u_{i,t}$:

$$[u_{i,t}] = -K_i c_i^{\frac{1}{2}} e^{\frac{1}{2}\int \beta_{ii}\,dx}. \tag{21}$$

(2) *Along* $dx/dt = -c_i$. In a similar way, the decay equations for the discontinuities of $u_{i,x}$ and $u_{i,t}$ can be obtained. They are

$$\begin{aligned}[u_{i,x}] &= K_i c_i^{-\frac{1}{2}} e^{\frac{1}{2}\int \beta_{ii}\,dx}\\ [u_{i,t}] &= K_i c_i^{\frac{1}{2}} e^{\frac{1}{2}\int \beta_{ii}\,dx}.\end{aligned} \tag{22}$$

3. FORMULATION OF THE PROBLEM

Our study is of a semi-infinite, cylindrical rod, of circular cross section, made of an isotropically elastic material. The rod is referred to a cylindrical coordinate system (r, θ, z) within which the center of the end of the rod is located at the origin and positive z is measured along the axis of the rod. We are concerned with axisymmetric motions of the rod and since our theory must involve only one space and one time variable we resort to an approximate theory. Our choice is the theory developed by Mindlin and McNiven [4] as it embraces a comparatively large frequency range and within that range duplicates the exact theory very closely. As it will be necessary to refer to it constantly we reproduce the essence of that theory here.

The theory is contained in the three equations

$$\begin{aligned}&\delta K_2^2(\delta u_{,xx}-4\psi_{,x})-8K_1^2(k^2-1)u-4K_1(k^2-2)\delta w_{,x}+\frac{4a}{\mu}R = K_3^2\delta^2 u_{,\tau\tau}\\ &\delta k^2 w_{,xx}+2K_1(k^2-2)u_{,x}+\frac{2a}{\delta\mu}Z = \delta w_{,\tau\tau}\\ &\delta^2 k^2\psi_{,xx}+6K_2^2(\delta u_{,x}-4\psi)-\frac{6a}{\mu}Z = \delta^2 K_4^2\psi_{,\tau\tau}.\end{aligned} \tag{23}$$

In equations (23); $R = \sigma_{r|r=a}$, $Z = \tau_{rz|r=a}$,

and

$$x = \frac{\delta z}{a}, \quad \text{a dimensionless distance}$$

$$\tau = \frac{\delta t}{a}\left(\frac{\mu}{\rho}\right)^{\frac{1}{2}}, \quad \text{a dimensionless time}$$

$$k^2 = \frac{2(1-\nu)}{(1-2\nu)},$$

where

δ a known constant
t time
a radius of the rod
μ shear modulus of elasticity
ρ mass density
ν Poisson's ratio.

The K_i's ($i = 1$–4) are adjustment factors introduced in the theory to make the three spectral lines of the theory match more closely the lowest three branches of the exact theory. They are functions only of Poisson's ratio, and have been extensively tabulated by Kaul and McCoy [3].

These tabulated values are based on matching the properties of the spectral lines from both the approximate and exact theories at cut off. This is not the only way that the spectral lines can be matched. Kaul and McCoy themselves suggested matching points on the complex branch, and as we are dealing here with stations near the end of the rod, this alternative was considered seriously. Study, however, showed that the additional effort involved on the alternate matching was unnecessary. The only frequencies on the complex branch that influence the motions near the end of the rod are frequencies in the neighborhood of the end mode [13]. For this neighborhood, with the adjustment factors used in this paper, the complex branches from both approximate and exact theories match almost perfectly.

The generalized displacements u, w and ψ in equations (23) are related to the radial and axial displacements u_r and u_z according to

$$\begin{aligned} u_r &\cong \alpha u(x, \tau) \\ u_z &\cong w(x, \tau) + (1 - 2\alpha^2)\psi(x, \tau), \end{aligned} \tag{24}$$

where $\alpha = r/a$; r is the radial distance.

The constitutive equations relating these generalized displacements and generalized forces are

$$\begin{aligned} \left(\frac{a}{\mu}\right) P_r &= 2K_1^2(k^2 - 1)u + \delta K_1(k^2 - 2)w_{,x} \\ 2\left(\frac{a}{\mu}\right) P_z &= \delta k^2 w_{,x} + 2K_1(k^2 - 2)u \\ 4\left(\frac{a}{\mu}\right) P_{rz} &= K_2^2(\delta u_{,x} - 4\psi) \\ 6\left(\frac{a}{\mu}\right) P_\psi &= \delta k^2 \psi_{,x}, \end{aligned} \tag{25}$$

where the generalized forces are defined by

$$\begin{aligned} P_r &= \int_0^1 (\sigma_r + \sigma_\theta)\alpha \, d\alpha \\ P_z &= \int_0^1 \sigma_z \alpha \, d\alpha \\ P_{rz} &= \int_0^1 \tau_{rz}\alpha^2 \, d\alpha \\ P_\psi &= \int_0^1 \sigma_z(1-2\alpha^2)\alpha \, d\alpha. \end{aligned} \tag{26}$$

Finally, the strains are given in terms of the generalized displacements according to

$$\begin{aligned} \varepsilon_r &= K_1 \frac{u}{a} \\ \varepsilon_\theta &= K_1 \frac{u}{a} \\ \varepsilon_z &= \frac{\delta}{a}\{w_{,x} + (1-2\alpha^2)\psi_{,x}\} \\ \varepsilon_{rz} &= K_2 \frac{\alpha}{2a}(\delta u_{,x} - 4\psi) \\ \varepsilon_{\theta z} &= \varepsilon_{r\theta} = 0. \end{aligned} \tag{27}$$

The authors of the approximate theory have shown that a unique solution will result when there is specified

(i) throughout the rod, the initial values of u, w, ψ and $\dot{u}$, $\dot{w}$, $\dot{\psi}$,
(ii) throughout the rod one member of each of the two products Ru and $Z(w-\psi)$,
(iii) at the end of the rod, one member of each of the three products $P_z w$, $P_\psi \psi$ and $P_{rz} u$.

We now proceed to formulate the problem in the context of the method of characteristics. Equations (23) take the form of equations (1) when

$$(\alpha_{ij}) = \begin{bmatrix} 0 & 0 & 0 \\ 0 & \dfrac{24K_2^2}{\delta^2 k^2} & 0 \\ 0 & 0 & \dfrac{8K_1^2(k^2-1)}{\delta^2 K_2^2} \end{bmatrix}$$

$$(\beta_{ij}) = \begin{bmatrix} 0 & 0 & \dfrac{-2K_1(k^2-2)}{\delta k^2} \\ 0 & 0 & \dfrac{-6K_2^2}{\delta k^2} \\ \dfrac{4K_1(k^2-2)}{\delta K_2^2} & \dfrac{4}{\delta} & 0 \end{bmatrix}. \tag{28}$$

Further, $(u_1, u_2, u_3) = (w, \psi, u)$ and

$$c_1^2 = k^2; \qquad c_2^2 = \frac{k^2}{K_4^2}; \qquad c_3^2 = \frac{K_2^2}{K_3^2}.$$

For a reasonable range of Poisson's ratio we assume that

$$c_1^2 > c_2^2 > c_3^2. \tag{29}$$

We note that $c_1 = k$ is the dimensionless form of the dilatational wave velocity $[(\lambda + 2\mu)/\rho]^{\frac{1}{2}}$.

Even though the method of characteristics is general and could be used to handle a large variety of boundary and initial conditions, we are concerned here with a specific problem, namely the response of a rod, initially at rest, whose cylindrical surface is free of traction, and subjected to a uniform pressure on the end of the rod that has an arbitrary dependence on time. The boundary conditions take the form;

$$\begin{aligned} R &= Z = 0 \\ \sigma_z(0, \tau) &= -f(\tau)H(\tau) \\ \tau_{rz}(0, \tau) &= 0. \end{aligned} \tag{30}$$

In equations (30) $H(\tau)$ is the usual Heaviside step function and $f(\tau)$ is a prescribed, continuous function of time.

In terms of the generalized forces the boundary conditions on the end of the rod can be written:

$$\begin{aligned} P_z(0, \tau) &= \frac{-f(\tau)H(\tau)}{2} \\ P_\psi(0, \tau) &= 0 \\ P_{rz}(0, \tau) &= 0. \end{aligned} \tag{31}$$

Using equations (25) these conditions can be expressed in terms of the generalized displacements according to

$$\begin{aligned} pw_{,x}(0, \tau) + qu(0, \tau) &= g(\tau)H(\tau) \\ \psi_{,x}(0, \tau) &= 0 \\ \delta u_{,x}(0, \tau) - 4\psi(0, \tau) &= 0, \end{aligned} \tag{32}$$

where

$$p = \frac{\delta k^2}{2}; \qquad q = K_1(k^2 - 2); \qquad g(\tau) = -\frac{af(\tau)}{2\mu}. \tag{33}$$

The initial conditions are

$$\begin{aligned} u(x, 0) &= u_{,\tau}(x, 0) = 0 \\ w(x, 0) &= w_{,\tau}(x, 0) = 0 \\ \psi(x, 0) &= \psi_{,\tau}(x, 0) = 0. \end{aligned} \tag{34}$$

The general problem is one of finding solutions of equations (23) subject to the boundary and initial conditions given by equations (32) and (34).

The rod behavior we are seeking is the response to an input of normal stress on the end of the rod. As the resulting disturbances will move down the rod, the behavior is best understood if it is described using the notion of wave fronts. The first wave front is defined as the boundary between disturbed and undisturbed regions of the rod, while second, third etc., wave fronts are related to the notion of the arrival of the additional disturbances to an already disturbed material point. When the material at a point becomes suddenly disturbed from an undisturbed state or when an already disturbed material point has some additional disturbance, it can only do so if some derivative of the displacement vector suffers a finite jump at the point. On the x–τ plane, a wave front can be represented by a line and by definition that line will be a characteristic. In our problem the initial conditions are all zero which means that of a family of characteristic lines, it is the ones emanating from the origin of the x–τ plane that will be the wave fronts. The order of discontinuity of the characteristic lines describing the wave fronts will depend on the boundary conditions on the end of the rod, specifically the dependence on time in the neighborhood of $\tau = 0$.

Since equations (23) represent three equations, there will be three wave fronts, S_1, S_2 and S_3, shown in Fig. 1. In the boundary conditions equations (30), $f(\tau)$ is an arbitrary continuous function of τ. If $f(0) \neq 0$, we will show shortly that along S_1 the first derivatives of w will suffer a finite jump, higher order derivatives of u and ψ will have a finite jump and that along S_2 and S_3 the discontinuities will be of order two or higher for all three generalized displacements. As S_1 is a characteristic line of first order discontinuity in w, it is necessary to use decay equations to find $w_{,x}$ and $w_{,\tau}$ along S_1 immediately behind the wave front.

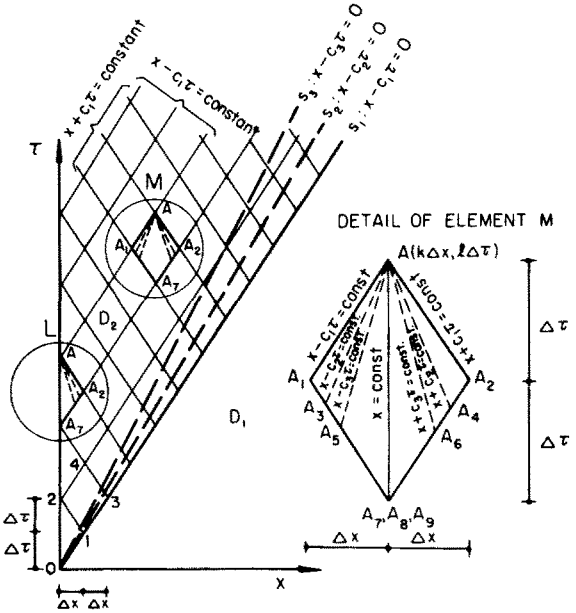

FIG. 1. Description of characteristic lines and wave fronts on the (x–τ) plane.

We turn to the decay equations themselves, equations (20), (21) and (22) as they apply to S_1, S_2 and S_3, and note from the second of equations (28) that $\beta_{11} = \beta_{22} = \beta_{33} = 0$. The decay equations are therefore,

$$\begin{aligned} [w_{,x}] &= A_1, \quad [w_{,\tau}] = -c_1 A_1 \quad \text{along } S_1 \\ [\psi_{,x}] &= A_2, \quad [\psi_{,\tau}] = -c_2 A_2 \quad \text{along } S_2 \\ [u_{,x}] &= A_3, \quad [u_{,\tau}] = -c_3 A_3 \quad \text{along } S_3. \end{aligned} \tag{35}$$

The A_i's are constants obtained from the behavior of the boundary and initial conditions in the neighborhood of the origin of the $(x$–$\tau)$ plane. Using boundary conditions equations (32) and initial conditions equations (34), and noting that $[u] = [w] = [\psi] = 0$ everywhere in the $(x$–$\tau)$ plane one obtains

$$\begin{aligned} [w_{,x}(0,0)] &= \frac{g(0)}{p} \\ [\psi_{,x}(0,0)] &= 0 \\ [u_{,x}(0,0)] &= 0. \end{aligned} \tag{36}$$

Comparing equations (35) and (36) we can identify

$$\begin{aligned} A_1 &= \frac{g(0)}{p} \\ A_2 &= A_3 = 0. \end{aligned} \tag{37}$$

Accordingly the decay equations are

$$\begin{aligned} [w_{,x}] &= \frac{g(0)}{p}, \quad [w_{,\tau}] = -\frac{c_1 g(0)}{p} \quad \text{along } S_1 \\ [\psi_{,x}] &= 0, \quad [\psi_{,\tau}] = 0 \quad \text{along } S_2 \\ [u_{,x}] &= 0, \quad [u_{,\tau}] = 0 \quad \text{along } S_3. \end{aligned} \tag{38}$$

It is worth noting that the Mindlin–McNiven theory indicates no decay of the first derivatives of the generalized displacements.

From equations (38) and from the fact that $f(\tau)$ is a continuous function of τ we conclude that in the disturbed region behind the wave front S_1, all of the first derivatives of the generalized displacements are continuous so that the canonical form of the equations are appropriate. Within the framework of the approximate theory these equations, equations (16), have the form,

$$\begin{aligned} \mp \mathrm{d}(w_{,x}) - \frac{1}{c_1}\mathrm{d}(w_{,\tau}) &= \mp \mathrm{d}x \beta_{13} u_{,x} && \text{along } \frac{\mathrm{d}x}{\mathrm{d}\tau} = \mp c_1 \\ \mp \mathrm{d}(\psi_{,x}) - \frac{1}{c_2}\mathrm{d}(\psi_{,\tau}) &= \mp \mathrm{d}x(\alpha_{22}\psi + \beta_{23} u_{,x}) && \text{along } \frac{\mathrm{d}x}{\mathrm{d}\tau} = \mp c_2 \\ \mp \mathrm{d}(u_{,x}) - \frac{1}{c_3}\mathrm{d}(u_{,\tau}) &= \mp \mathrm{d}x(\alpha_{33} u + \beta_{31} w_{,x} + \beta_{32}\psi_{,x}) && \text{along } \frac{\mathrm{d}x}{\mathrm{d}\tau} = \mp c_3. \end{aligned} \tag{39}$$

Along with the six equations of equations (39) we exploit the fact that the displacement field is continuous and differentiable, so that along any line on the x–τ plane

$$\begin{aligned} dw &= w_{,x}\,dx + w_{,\tau}\,d\tau \\ d\psi &= \psi_{,x}\,dx + \psi_{,\tau}\,d\tau \\ du &= u_{,x}\,dx + u_{,\tau}\,d\tau \end{aligned} \tag{40}$$

giving us nine working equations.

4. NUMERICAL ANALYSIS

We seek the generalized displacements u, ψ and w and their first derivatives at a station x and at a time τ, and having these we can calculate the strains and stresses. We refer to Fig. 1, which shows the $(x$–$\tau)$ plane. On this plane, the line $S_1(x - c_1\tau = 0)$ divides the space–time domain into two parts, the domain D_1 representing undisturbed particles and D_2 representing particles of the rod which are in motion. The part D_2, which is the part that interests us, is subdivided by means of one primary and two secondary grids. The primary grid shown by fine solid lines is formed by two sets of parallel lines. The first set ($x - c_1\tau$ = const) is parallel to the line S_1, and second set ($x + c_1\tau$ = const) has equal but opposite slopes. Each diamond shaped element has diagonals measuring $2\Delta x$ and $2\Delta\tau$. The secondary sets of grid lines are members of the families $x \pm c_2\tau$ = constant and $x \pm c_3\tau$ = constant. They are shown dotted in Fig. 1, and are used when analyzing an individual element. As the dotted lines fall within the element, the domain of dependence of a point is conserved.

In what follows the nine quantities u, $u_{,x}$, $u_{,\tau}$, ψ, $\psi_{,x}$, $\psi_{,\tau}$, w, $w_{,x}$, $w_{,\tau}$ are considered, for convenience, to be the nine elements of the vector y_i. To establish y_i in the region D_2, we start at the origin and along S_1, where it is known, and fan out into the region element by element. To be more explicit, we know y_i at the points 0 and 1 in Fig. 1, and using a technique to be explained shortly, we find y_i at the point 2. Having y_i at the points 1, 2 and 3, we use the same technique to find y_i at the point 4, and so forth.

In explaining the technique we refer to element M shown in Fig. 1, and to its detached enlargement. y_i is known at points A_1, A_7 and A_2 and is sought at the point A. As there are nine unknowns, we need nine equations to establish them.

The boundary lines AA_1 and AA_2 are the characteristic lines $x_1 - c_1\tau$ = constant, and $x + c_1\tau$ = constant respectively. Through the point A we draw the characteristic lines AA_3 and AA_4 with slopes $\pm c_2$, and characteristic lines AA_5 and AA_6 with slopes $\pm c_3$. The values of y_i are calculated at A_3 and A_5 by interpolating the values at A_1 and A_7, and at A_4 and A_6 by interpolating the values at A_7 and A_2. Six of the nine equations come from using six canonical equations, equations (39), one each along the six characteristic lines per element converging on A.

The three remaining equations are equations (40). As these are valid for any line on the $(x$–$\tau)$ plane, we choose to use them along the diagonal line AA_7 (x = constant). The nine elements of y_i are found at A by solving the nine equations by the method of finite differences.

For an element L adjacent to the line $x = 0$, the procedure is the same except that the three equations along the three lines $x - c_i\tau$ = constant ($i = 1, 2, 3$) must be replaced by

the end boundary conditions at $x = 0$, equations (32);

$$\begin{aligned} pw_{,x}(A) + qu(A) &= g(A) \\ \psi_{,x}(A) &= 0 \\ \delta u_{,x}(A) - 4\psi(A) &= 0. \end{aligned} \tag{41}$$

When one is dealing with numerical methods of this kind, convergence must be considered. In the Appendix we show that for fixed point (x^*, τ^*) on the $(x-\tau)$ plane, the error becomes zero as the mesh size $\Delta\tau$ goes to zero.

5. NUMERICAL RESULTS

Our choice is to calculate and exhibit three quantities; the radial strain ε_r and the axial force P_z for comparison with other published results and the axial strain ε_z which can be checked against future experiments. For an input on the end of the rod we choose $f(\tau) =$ a constant P_0. With the method of characteristics $f(\tau)$ can be an arbitrary function and this particular choice was made for two reasons; first, so that we could compare the results with those obtained by Bertholf [9] and second, because of the limitations of the approximate theory. As the Mindlin–McNiven theory is limited to frequencies less than that of the cut-off frequency of the second axial shear mode, it is advisable to choose an input function for which the magnitude of its Fourier transform decreases with increasing frequency. The Fourier transform of P_0 decreases as $(1/\omega)$ with increasing frequency.

The rod is assumed to have a Poissons ratio of 0·29. The numerical analysis was carried using a mesh size dictated by $\Delta x = 0{\cdot}10$. The response was evaluated at two stations; the first at $x = 7{\cdot}60$, about 1 dia., and at $x = 15{\cdot}20$, about 2 dia. from the end of the rod. The responses are in Figs. 2–5. The approximate theory accommodates a distribution of the axial strain across a rod cross section and so Figs. 3(a) and 3(b) show a prediction of this strain at the center of the rod as well as on its lateral surface. It should be noted from the figures that at any station, ε_r, ε_z and P_z asymptotically approach their static values as time increases indefinitely, which ensures the stability of the numerical procedure.

We have attempted to appraise the numerical results three separate ways, with varying degrees of success. The first way is by comparison with published results of experiments. The best experiments were carried out by Miklowitz and Nisewanger [14] though the best report of the experiments appears in the paper by Bertholf [9] no doubt after private communication with the authors.

The comparisons can be seen in the figures; we will compare radial and axial strains separately. The radial strains are shown in Figs. 2(a) and 2(b) at two separate stations. The figures show that the predicted and experimental responses have approximately the same peak value but that the head of impulse for our theoretical response is steeper than the experimental. In Fig. 3(a) we see that the axial strains on the lateral surface predicted by our theory and recorded in experiments differ both at the head of impulse and behind it.

The second comparison is with the numerical results presented by other authors. Comparison is valid with only two of these because all of the others formulated their theory using integral transforms, found it necessary to use the method of steepest descent in their numerical analysis, and so calculated the response at stations far from the end of the rod, whereas ours was calculated close to the end.

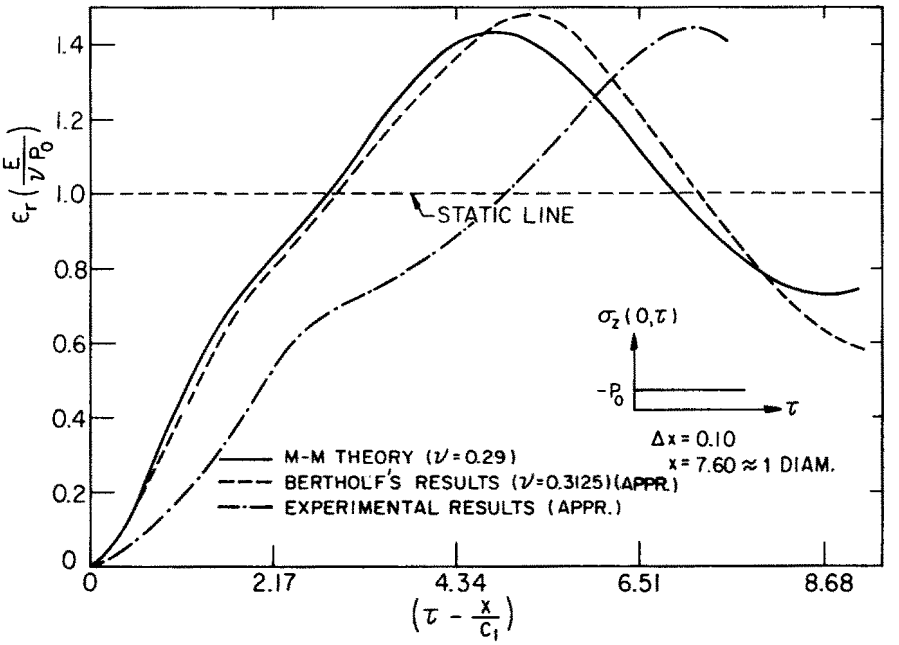

FIG. 2(a). Radial strain for the station $z \approx 1$ dia.

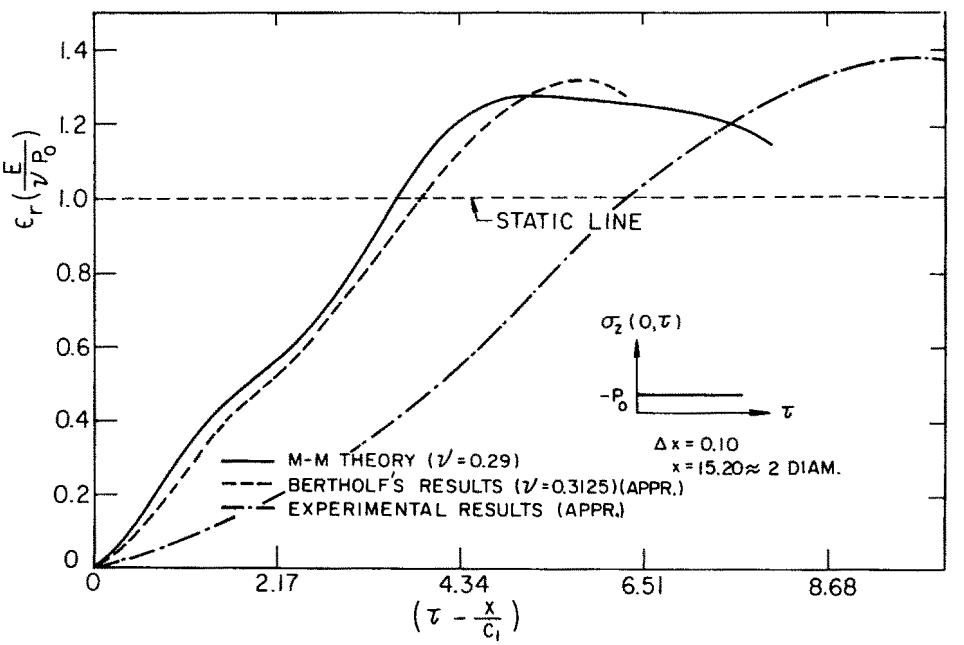

FIG. 2(b). Radial strain for the station $z \approx 2$ dia.

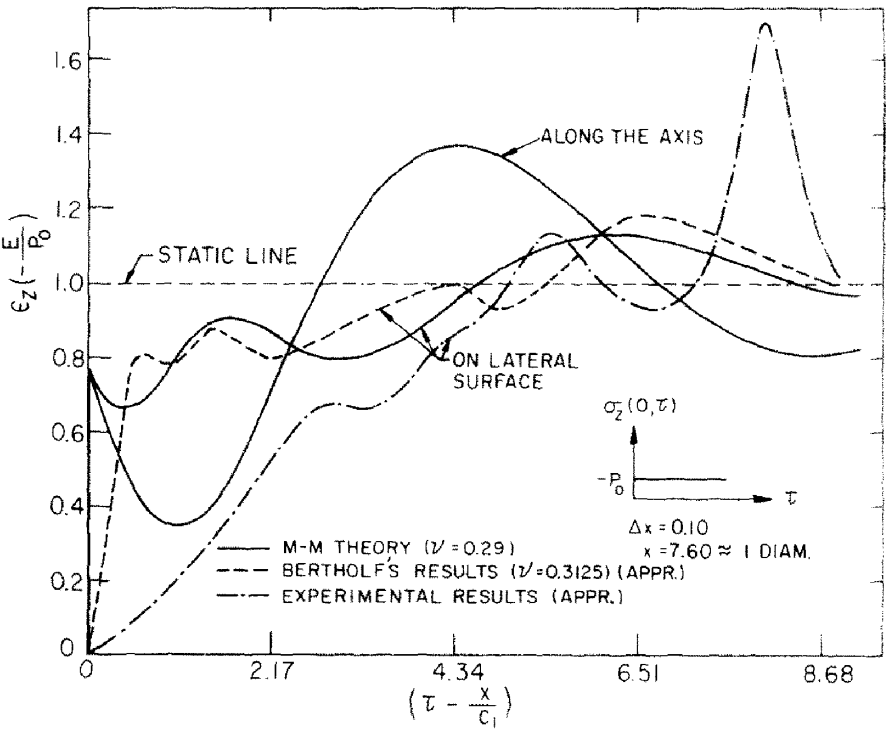

FIG. 3(a). Axial strain for the station $z \approx 1$ dia.

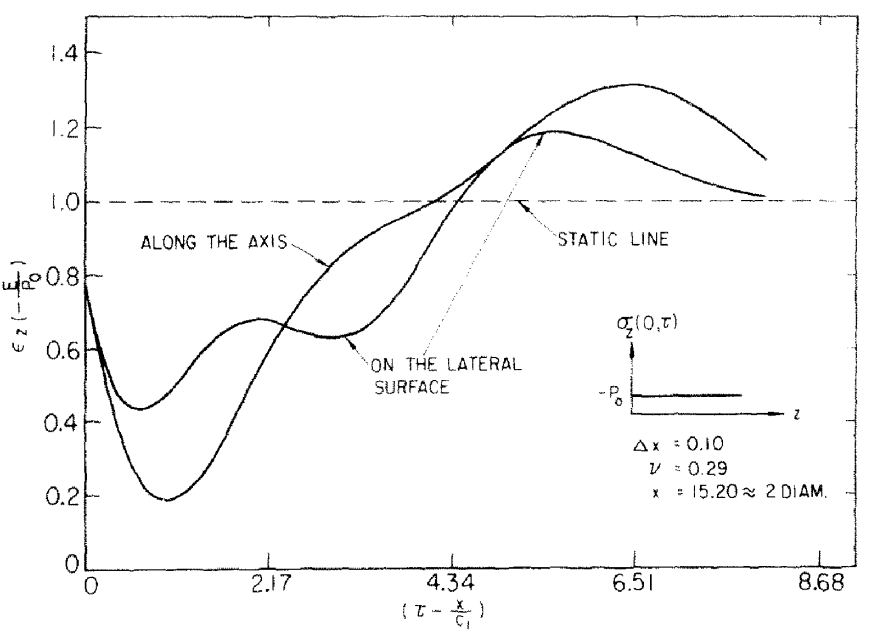

FIG. 3(b). Axial strain for the station $z \approx 2$ dia.

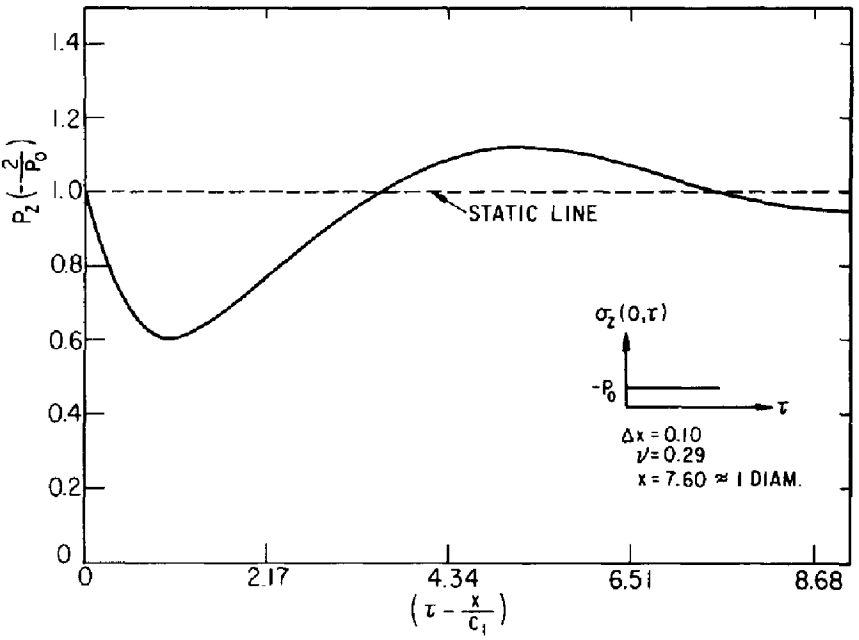

FIG. 4(a). Axial generalized force for the station $z \approx 1$ dia.

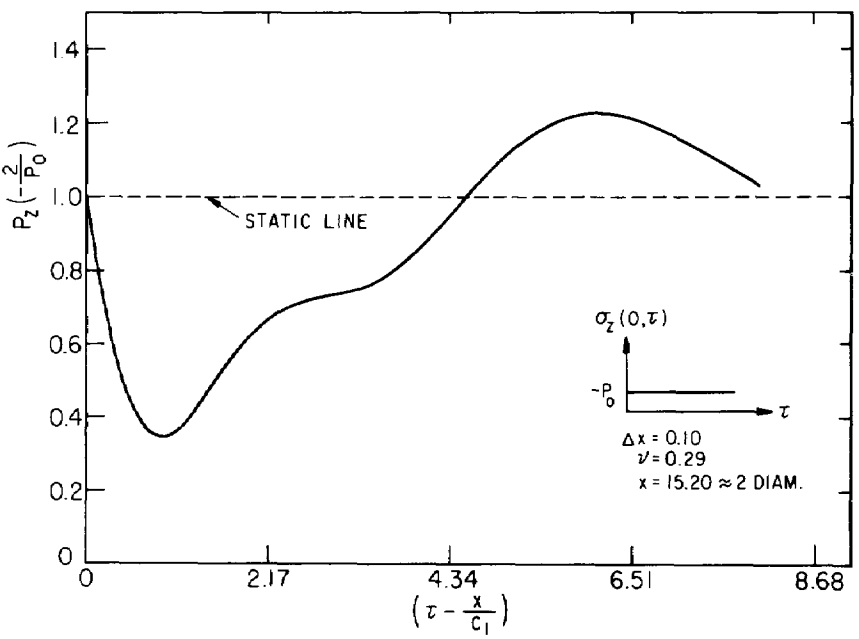

FIG. 4(b). Axial generalized force for the station $z \approx 2$ dia.

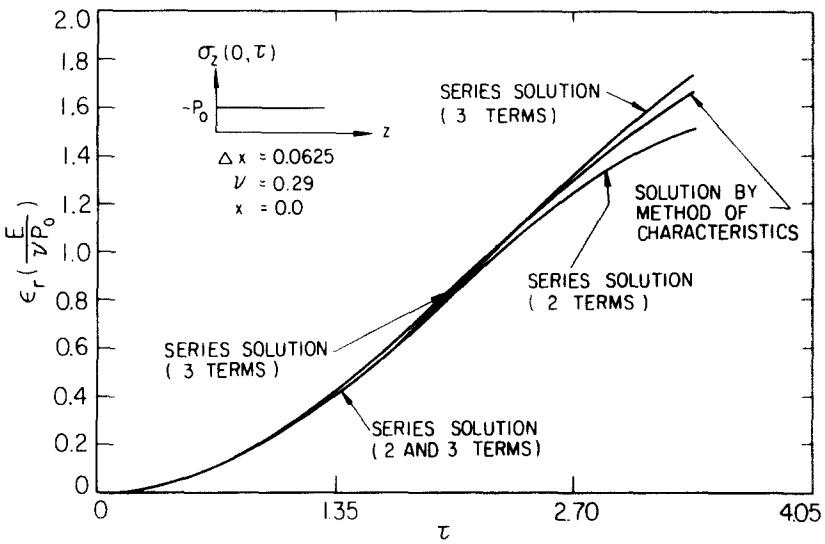

FIG. 5. Comparison of radial strain found using the methods characteristics and series expansion.

Of the two that calculated the response close to the end of the rod, the earliest work was by Miklowitz [7]. His work differed from ours in three respects; he used different values of Poisson's ratio (0·244, 0·325), he adopted mixed–mixed conditions on the end of the rod, and based his work on the theory due to Mindlin and Herrmann [8] rather than Mindlin and McNiven [4] which came later. Because we were interested in making a comparison with Miklowitz we ran a computation using his Poisson's ratios and end conditions for the quantity P_z. For the case $\nu = 0{\cdot}244$ the match over a limited time range is good. The first amplitude and half period match exactly. For the case $\nu = 0{\cdot}325$ the match of the same quantities is just fair. We speculate that the difference in matching is due to the shortcomings of the Mindlin–Herrmann theory. When $\nu = 0{\cdot}244$ it is less than $\nu_c = 0{\cdot}2833$, the "critical" value, so that the second mode is the radial mode the only higher mode in the Mindlin–Herrmann theory, whereas when $\nu = 0{\cdot}325$ the second mode is not the radial mode making the theory less appropriate for this case.

The other pertinent numerical results are due to L. D. Bertholf [9]. He used the three-dimensional theory of elasticity, solving the equations by finite differences. The numerical analysis, while appropriate, seems to us to have a mathematical weakness. Bertholf apparently did not take into account the notion of the domain of dependence for hyperbolic equations which puts restriction on the selection of the time mesh size as a function of the space mesh size. In spite of this reservation concerning his results and the slight difference in the two Poisson's ratios (he used $\nu = 0{\cdot}3125$), we compared the numerical results for the radial strain ε_r and the axial strain ε_z on the surface.

The comparisons can be seen in Figs. 2(a), 2(b) and 3(a). The closeness of the two radial strain responses seen in both Figs. 2(a) and 2(b) helps to give confidence that the predicted are close to the true responses. In Fig. 3(a) the axial strain responses along the axis of the rod and on the lateral surface must be considered separately. The jump in ε_z along the axis of the rod at the head of impulse is correct and consistent with the three dimensional

exact theory as discussed by Tang and Yen [15]. Apart from the head of impulse we have nothing with which to compare the strain along the axis.

The responses of axial strain on the lateral surfaces predicted by Bertholf and ourselves are fairly close to one another except at the head of impulse. For this part of the response Bertholf is closer to the truth. There is no jump in ε_z at the head of impulse as our response shows. It is likely that the time response is close to the functional form $(t-z/V_1)^{\frac{1}{2}}$, V_1 being dilatational wave velocity, suggested by Rosenfeld and Miklowitz [16].

The third method used for appraising the results is one developed by the authors and will be presented in detail in a forthcoming paper. The method consists of using the same approximate theory, the same conditions on the end of the rod and initial conditions, but of expanding the solution in terms of a power series in time about the wave fronts. Here, it is used to appraise the radial strain at the end of the rod, $x = 0$. The series has the form

$$\varepsilon_r = A_2\tau^2 - A_4\tau^4 + A_6\tau^6, \tag{42}$$

where all of the A_{2n}'s are positive. The method makes a powerful tool for judgment because the series converges very quickly and for a particular truncation one is able to judge closely how the succeeding term would improve the answer. If we examine Fig. 5 we see first the radial strain response if we use two terms of the expansion. We also know that the third term in the expansion is positive and if it is used we get higher values of ε_r also shown. We also know that if the fourth term were used it would be negative and smaller than the third so that, if included, the strain would be lower than that for 3 terms but closer to the 3 term curve than to the 2 term curve. As the series converges quickly one can conclude that the radial strain response using the method of characteristics is very close to where it would be if a large number of terms of the expansion were used, the correct response within the limits of the approximate theory.

Acknowledgment—This study was sponsored by a Grant provided to the University of California by the National Science Foundation.

REFERENCES

[1] R. Skalak, *J. appl. Mech.* **79**, 59 (1957).
[2] R. Folk, G. Fox, C. A. Shook and C. W. Curtis, *J. acoust. Soc. Am.* **30**, 552 (1958).
[3] R. K. Kaul and J. J. McCoy, *J. acoust. Soc. Am.* **36**, 653 (1964).
[4] R. D. Mindlin and H. D. McNiven, *J. appl. Mech.* **82**, 145 (1960).
[5] O. E. Jones and F. R. Norwood, *J. appl. Mech.* **89**, 718 (1967).
[6] J. R. Lloyd and J. Miklowitz, *Proc. 4th natn. Congr. appl. Mech.* p. 255 (1962).
[7] J. Miklowitz, *J. appl. Mech.* **24**, 231 (1957).
[8] R. D. Mindlin and G. Herrmann, *Proc. 1st. Congr. appl. Mech.* p. 187 (1952).
[9] L. D. Bertholf, *J. appl. Mech.* **89**, 725 (1967).
[10] S. C. Tang, *AIAA Jnl.* **3**, 1174 (1965).
[11] P. C. Chou and R. W. Mortimer, *J. appl. Mech.* **89**, 745 (1967).
[12] R. Courant and D. Hilbert, *Method of Mathematical Physics*, vol. II. Interchange (1966).
[13] H. D. McNiven, *J. acoust. Soc. Am.* **33**, 23 (1961).
[14] J. Miklowitz and C. R. Nisewanger, *J. appl. Mech.* **24**, 240 (1957).
[15] S. C. Tang and D. H. Y. Yen, *J. appl. Mech.* **80**, 199 (1968).
[16] R. L. Rosenfeld and J. Miklowitz, *Proc. 4th natn. Congr. appl. Mech.* p. 293 (1962).
[17] Richard Courant, Eugene Isaacson and Mina Rees, *Communs. pure appl. Math.* V, 243 (1952).

APPENDIX

Convergence proof for the numerical method

The proof is modeled after a more general proof due to R. Courant *et al.* [17], concerning the finite difference method as it applies to the canonical form of quasilinear hyperbolic equations along the characteristics using rectangular and curvelinear networks.

The proof begins by letting

$$u_i = (w_{,x}, w_{,t}, \psi_{,x}, \psi_{,t}, u_{,x}, u_{,t}, w, \psi, u). \tag{A-1}$$

The equations along the characteristics then have the form

$$a_{ij}\frac{\mathrm{d}u_j}{\mathrm{d}\tau} = b_{ij}u_j \tag{A-2}$$

where:

$$i = 1, 2 \text{ along characteristics } \frac{\mathrm{d}x}{\mathrm{d}\tau} = \pm c_1$$

$$i = 3, 4 \text{ along characteristics } \frac{\mathrm{d}x}{\mathrm{d}\tau} = \pm c_2$$

$$i = 5, 6 \text{ along characteristics } \frac{\mathrm{d}x}{\mathrm{d}\tau} = \pm c_3$$

$$i = 7, 8, 9 \text{ along characteristics } \frac{\mathrm{d}x}{\mathrm{d}\tau} = 0.$$

and a_{ij} and b_{ij} are constants.

We discretize the $(x$–$\tau)$ plane with the network shown in Fig. 1 so that the point (k, l) corresponds to the point with coordinates $x = k\Delta x$, $\tau = l\Delta\tau$. Let y_i be the finite difference solution of equation (A-2), i.e.

$$a_{ij}\frac{y_j(A) - y_j(A_i)}{s_i\Delta\tau} = b_{ij}y_j(A) \quad \text{(no sum on } i\text{)} \tag{A-3}$$

where $1 \le s_i \le 2$.

Using interpolation, $y_j(A_i)$ is expressed in terms of $y_j(A_7)$ and $y_j(A_1)$ or $y_j(A_2)$ (Fig. 1), i.e.

$$y_j(A_i) = \alpha_i y_j(A_7) + \beta_i y_j(A_1 \text{ or } A_2) \tag{A-4}$$

where α_i, β_i are interpolation constants with

$$\alpha_i + \beta_i = 1, \qquad \alpha_i \ge 0, \qquad \beta_i \ge 0.$$

Substitution of equation (A-4) into equation (A-3) gives:

$$a_{ij}y_j(A) = s_i\Delta\tau b_{ij}y_j(A) + a_{ij}[\alpha_i y_j(A_7) + \beta_i y_j(A_1 \text{ or } A_2)] \quad \text{(no sum on } i\text{)}. \tag{A-5}$$

Let p_i be the exact solution of equation (A-2): i.e.

$$a_{ij}\frac{p_j(A) - p_j(A_i)}{s_i\Delta\tau} + O_i(\Delta\tau) = b_{ij}p_j(A) \tag{A-6}$$

with

$$p_j(A_i) = \alpha_i p_j(A_7) + \beta_i p_j(A_1 \text{ or } A_2) + O_j(\Delta\tau^2). \tag{A-7}$$

Substitution of equation (A-7) into equation (A-6) gives:

$$a_{ij}p_j(A) = s_i\Delta\tau b_{ij}(A) + a_{ij}[\alpha_i p_j(A_7) + \beta_i p_j(A_1 \text{ or } A_2)] + O_i(\Delta\tau^2) \quad \text{(no sum on } i\text{)}. \tag{A-8}$$

Taking the difference of equations (A-5) and (A-8), one finds:

$$a_{ij}v_j(A) = s_i\Delta\tau b_{ij}v_j(A) + a_{ij}[\alpha_i v_j(A_7) + \beta_i v_j(A_1 \text{ or } A_2)] + O_i(\Delta\tau^2) \quad \text{(no sum on } i\text{)} \tag{A-9}$$

where $v_j = p_j - y_j$.

Or,

$$a_{ij}v_j^{k,l} = s_i\Delta\tau b_{ij}v_j^{k,l} + a_{ij}(\alpha_i v_j^{k,l-2} + \beta_i v_j^{k-1 \text{ or } k+1,l-1}) + O_i(\Delta\tau^2) \quad \text{(no sum on } i\text{)} \tag{A-10}$$

where

$$v_j^{k,l} = v_j(k\Delta x, l\Delta\tau) \text{ (Fig. 1)}.$$

From equation (A-10), one finds

$$|a_{ij}v_j^{k,l}| \le s_i\Delta\tau|b_{ij}v_j^{k,l}| + |a_{ij}(\alpha_i v_j^{k,l-2} + \beta_i v_j^{k-1 \text{ or } k+1,l-1})| + |O_i(\Delta\tau^2)| \quad \text{(no sum on } i\text{)}. \tag{A-11}$$

Let us introduce the measure of error as

$$E_l^k = \max_i |a_{ij}v_j^{k,l}|. \tag{A-12}$$

Then, from equations (A-11) and (A-12) one obtains

$$E_l^k \le \beta_1\Delta\tau E_l^k + a_1 E_{l-2}^k + a_2 E_{l-1}^{k-1 \text{ or } k+1} + \beta_2\Delta\tau^2, \tag{A-13}$$

where $\beta_1, \beta_2, a_1, a_2$ are positive constants with $a_1 + a_2 = 1$. Equation (A-13) is the governing equation for the growth of the error. Using equation (A-13), together with the boundary and initial conditions, one obtains:

$$E_l^k < \frac{\beta_2\Delta\tau^2}{1-\beta_1\Delta\tau}\sum_{n=0}^{l-1}\frac{1}{(1-\beta_1\Delta\tau)^n}$$

or

$$E_l^k < \frac{\beta_2\Delta\tau^2}{1-\beta_1\Delta\tau}\,\frac{1-1/(1-\beta_1\Delta\tau)^l}{1-1/(1-\beta_1\Delta\tau)}$$

or

$$E_l^k < -\frac{\beta_2\Delta\tau}{\beta_1}\left[1-\frac{1}{(1-\beta_1\Delta\tau)^l}\right]$$

Putting $\Delta\tau = \tau/l$, one finds

$$E_l^k < -\frac{\beta_2\tau}{\beta_1 l}\left[1-\frac{1}{[1-\beta_1(\tau/l)]^l}\right]. \tag{A-14}$$

Now, we let

$$H_l^k = -\frac{\beta_2\tau}{\beta_1 l}\left[1-\frac{1}{[1-\beta_1(\tau/l)]^l}\right]. \tag{A-15}$$

For fixed values of (x, τ), and taking limit of equation (A-15) as l goes to infinity (this is equivalent to letting $\Delta\tau \to 0$), one finds:

$$\lim_{l\to\infty} H_l^k = -\lim_{l\to\infty} \frac{\beta_2\tau}{\beta_1 l}\left[1 - \frac{1}{[1-\beta_1(\tau/l)]^l}\right]$$

or (A-16)

$$\lim_{l\to\infty} H_l^k = -\lim_{l\to\infty} \frac{\beta_2\tau}{\beta_1 l}\left[1 - \frac{1}{e^{-\beta_1\tau}}\right] = 0.$$

Therefore, we conclude that for a fixed point (x^*, τ^*) on the $(x-\tau)$ plane, the error becomes zero as the mesh size $\Delta\tau$ goes to zero. Hence, the convergence of the numerical procedure used in this paper is established.

(*Received* 13 *June* 1969; *revised* 30 *October* 1969)

Абстракт—Используя метод характеристик, определяется поведение полубесконечного, изотропного, упругого стержня под влиянием импульса, зависящего от времени и приложенного на его конце. Применяется приближенная теория Миндлина и Мак Нивена для сведения задачи к такой, в которой движения зависят только от пространственной координаты и времени. Определяется поведение стержня в точках близи его конца для ступенчатого импульса давления. Сравнивается с резуиомемциц приводимыми в других опубликованных работах и с резуимемои авторов, найденным независимо.